DALTON
FULL PAPER

Chemical excision from amorphous MoS_3; a quantitative EXAFS study

Simon J. Hibble,* Mark R. Feaviour and Matthew J. Almond

Department of Chemistry, University of Reading, Whiteknights, Reading, UK RG6 6AD. E-mail: s.j.hibble@rdg.ac.uk

Received 16th October 2000, Accepted 22nd January 2001
First published as an Advance Article on the web 22nd February 2001

Quantitative information on the molybdenum containing species produced by the reaction of aqueous cyanide with the amorphous molybdenum sulfide MoS_3 has been obtained from extended X-ray absorption fine structure (EXAFS) studies. The results of this chemical excision study, in which Mo–Mo bonded triangular clusters are extracted from the solid, suggest that 70% of the molybdenum present in MoS_3 is found in Mo_3 clusters. This result is consistent with earlier diffraction and EXAFS experiments, but rules out the simplistic models proposed in those studies.

Introduction

Amorphous MoS_3 has attracted widespread interest from both academic and industrial researchers.[1–14] In addition to curiosity about the structure of an apparently simply binary sulfide, the fact that MoS_2 is used industrially as a hydrodesulfurisation catalyst, and MoS_3 has been implicated as a precursor to the poorly crystalline MoS_2 which is active in this reaction,[1,2] has led to a significant effort to determine its structure. MoS_3 has also attracted attention as a battery cathode material in lithium cells.[3] There is however, in spite of the large number of structural studies carried out using EXAFS,[4–7] X-ray[8–10] and neutron diffraction,[11] no consensus on the structure of amorphous MoS_3.

The two most popular structural models are the chain model, in which MoS_6 octahedra share faces to form chains with Mo–Mo bonds between alternate pairs of molybdenum atoms, and models based on Mo–Mo bonded Mo_3 triangles. The latter model is attractive to chemists because a large number of molybdenum(IV)–sulfur species containing Mo_3 clusters are known and the $[Mo_3S_4]^{4+}$ and $[Mo_3S_7]^{4+}$ cores, Fig. 1, occur in a large number of compounds, for example $K_5[Mo_3S_4(CN)_9]\cdot 3KCN\cdot 4H_2O$[14] and $[NH_4]_2[Mo_3S_{13}]$.[15] However, molybdenum sulfur species containing Mo–Mo dimers are also known, for example in the Mo^V containing compound $[NH_4]_2[Mo_2S_{12}]\cdot 2H_2O$.[16]

Müller has used chemical methods in an attempt to gain further information on the structure of MoS_3. He has claimed that, because the reaction of OH^- and CN^- with MoS_3 produces Mo_3 triangular clusters[12,13] these units must be present in the amorphous solid. In an elegant mass spectrometry experiment using $^{92}MoS_3$ and $^{100}MoS_3$, Müller *et al.* demonstrated that the molybdenum atoms in the Mo_3 clusters were not formed from Mo and Mo_2 species in solution,[14] but must come directly from the parent solid. Others[1] have taken the results from Müller's work and constructed models for the structure of amorphous MoS_3 built solely from Mo_3 clusters. We were concerned that these models were derived from yields of molybdenum species that are not known accurately, because they had been measured long after the initial reaction with the solid, and only on the precipitated molybdenum complexes.

We have used molybdenum K-edge EXAFS studies combined with UV-visible spectroscopy to determine the molybdenum species formed in solution by the reaction of aqueous cyanide with amorphous MoS_3, and to follow the evolution of species as a function of time. We chose to study the excision reaction with aqueous cyanide because the molybdenum sulfide is digested rapidly and all subsequent reactions take place in solution. Müller has studied the reactions of cyanide with molybdenum sulfides extensively, and demonstrated that the reactions shown in Fig. 2 take place.[17,18]

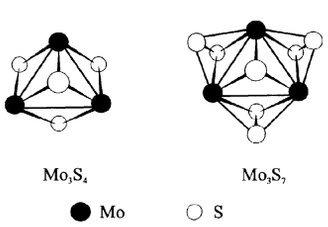

Fig. 1 The Mo–Mo bonded triangles in the Mo_3S_4 and Mo_3S_7 cores.

Experimental

Sample preparation

Molybdenum trisulfide dihydrate, $MoS_3\cdot 2H_2O$, was prepared by adding concentrated HCl to an aqueous solution of $[NH_4]_2[MoS_4]$ (66 mmol dm^{-3}) until the pH became 1. The resulting black precipitate was separated from the mixture by filtration, washed with water, EtOH, Et_2O and dried *in vacuo*.

The reaction and sampling

34 cm^3 of aqueous KCN (BDH) solution (900 mmol dm^{-3}) were placed in an Erlenmeyer flask on a thermostatted hot plate and the temperature raised to 60 °C. The molybdenum sulfide, 0.77 g of $MoS_3\cdot 2H_2O$, was then added to initiate the reaction.

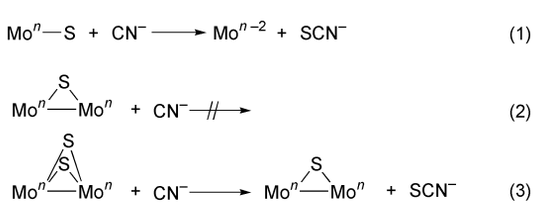

Fig. 2 Reactions of molybdenum–sulfide units with cyanide (after Müller[17,18]).

This gave a 9 : 1 molar ratio of CN^- to molybdenum and a solution approximately 100 mmolar in molybdenum. The solid appeared to have dissolved within 5 minutes. The flask was covered with a watch glass and the reaction followed over 46 hours. Periodically small aliquots ≈0.5 cm^3 of the solution were withdrawn and injected into solution sample cells for molybdenum K-edge EXAFS experiments. At the same time 1 cm^3 samples were withdrawn for UV-visible spectroscopy. In addition, a few drops of solution were withdrawn for infrared spectroscopy at fifteen minutes after the start of the reaction and also after 48 hours.

Spectroscopy

Infrared spectra were obtained by adding a few drops of reaction solution to finely powdered KBr (*ca.* 0.5 g). The resulting pastes were washed in EtOH, dried *in vacuo* and pressed into pellets. Spectra recorded using a Perkin-Elmer 1720-X interferometer. Aliquots of the reaction solution (1 cm^3) were diluted 250 times with water and their UV-visible spectra recorded on a Cary UV-visible spectrophotometer in quartz cells with a path length of 1 cm.

EXAFS experiment and data analysis

Molybdenum K-edge EXAFS data were collected in transmission mode on station 9.2 at the Daresbury Laboratory SRS operating with an average stored energy of 2 GeV and a typical electron current of 200 mA. EXAFS data were collected over a period of 10 minutes in QuEXAFS mode using a rapidly scanning Si (220) monochromator. Ionisation chambers, filled with a mixture of Ar–He or Xe–He at appropriate partial pressures to optimise detector sensitivities, were placed in the beam path before and behind the sample. The sample solutions were contained in 4 mm thick Perspex cells between polyester film (Mylar (30 μm thick, Goodfellow)) windows held in place by Araldite™. The monochromator was calibrated by scanning the molybdenum K-edge of a molybdenum foil and adjusted to give 60% harmonic rejection.

The raw EXAFS data were processed using the program EXCALIB[19a] and the position of the absorption edge determined from the derivative of the spectrum using EXBROOK.[19b] This program was also used to carry out background subtraction in order to extract the EXAFS data $\chi(k)$. Least-squares fitting of the k^3 weighted EXAFS data was carried out using the EXCURV 98[19c] program employing curved wave theory and using Hedin–Lindquist ground states and von Barth exchange potentials to calculate appropriate phase shifts and backscattering amplitudes. It was necessary to include multiple scattering into the EXAFS data analysis to account for backscattering from the nearly linear Mo–C–N unit. This was achieved using the curved wave theory option available in EXCURV 98. The quality of fit is reported relative to the discrepancy index $R = (\int|\chi_i^{calc}(k) - \chi_i^{exp}(k)|k^3 dk / \int|\chi_i^{exp}(k)|k^3 dk) \times 100\%$ where χ_i^{calc} and χ_i^{exp} are the ith data points of the calculated and experimental X-ray absorption coefficient, respectively. EXAFS spectra were Fourier transformed to produce a one-dimensional radial distribution function, using phase shifts calculated for the first atomic shell.

Results and discussion

Preliminary analysis of the UV-visible spectra, Fig. 3, and EXAFS data, Fig. 4, showed that after 46 hours the solution produced by the reaction between MoS_3 and aqueous CN^- contained two molybdenum containing species $[Mo_3S_4(CN)_9]^{5-}$ (≈70%) and $[MoO_4]^{2-}$ (≈30%). The amount of Mo found as the $[Mo_3S_4(CN)_9]^{5-}$ species was calculated from the UV-visible spectrum using the absorption coefficient, $\varepsilon_{378} = 5347\ M^{-1}\ cm^{-1}$, determined from a solution of $K_5[Mo_3S_4(CN)_9]\cdot 2H_2O$. Assuming that no other species was absorbing at 378 nm this

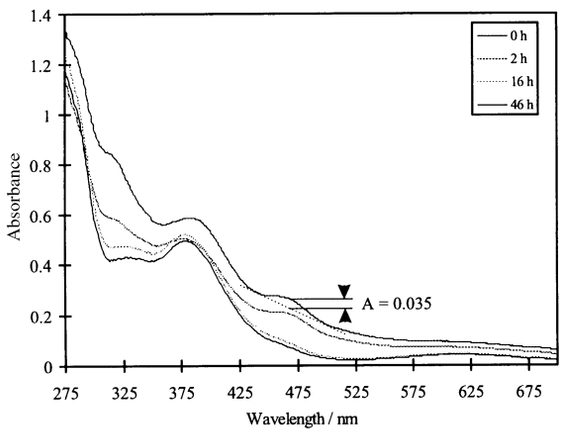

Fig. 3 UV-visible spectra of the solution produced by the reaction of MoS_3 and aqueous KCN at 0, 2, 16 and 46 hours.

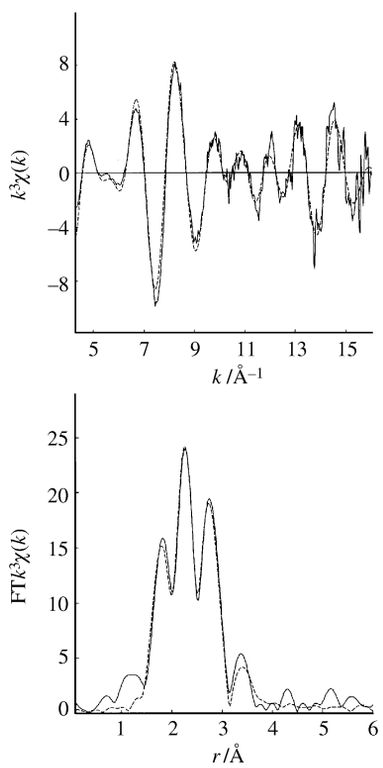

Fig. 4 Molybdenum K-edge EXAFS for MoS_3 + CN^- after 46 hours. Top: k^3-weighted EXAFS, (—) experimental and (----) theoretical. Bottom: the Fourier transforms.

gave a figure of 69% for the percentage of molybdenum in MoS_3 converted into $[Mo_3S_4(CN)_9]^{5-}$.

The Fourier transform of the molybdenum K-edge EXAFS obtained after 46 hours exhibits four peaks (Fig. 4) which, moving from low to high r, correspond to the Mo–O, overlapping Mo–S and Mo–C, Mo–Mo and Mo–(C)–N shells respectively in the two species $[MoO_4]^{2-}$ and $[Mo_3S_4(CN)_9]^{5-}$. Using the EXAFS data for the solution after 46 hours the percentage of molybdenum in the form of $[Mo_3S_4(CN)_9]^{5-}$ was calculated to be 75 ± 17%, and that in $[MoO_4]^{2-}$ as 33 ± 3%.

Our experimental results disagree with those of Weber *et al.*[1] who found only 35% of the molybdenum in MoS_3 was converted into $[Mo_3S_4(CN)_9]^{5-}$, but this was based on measuring the yield of solid $K_5[Mo_3S_4(CN)_9]\cdot 2H_2O$ rather than directly on the solution.

Determining and quantifying the molybdenum species formed in the initial stage of the reaction was more problematical. From the UV-visible spectrum at $t = 0$ shown in Fig. 3, it

Table 1 Structural parameters obtained from the molybdenum K-edge EXAFS study of the reaction between MoS_3 and KCN in aqueous solution (Model A)

Time/h	N_O	N_C	A_C/Å^2	N_S	A_S/Å^2	N_{Mo}	A_{Mo}/Å^2	A_N/Å^2
0	0.00	2.6(1.1)	0.005(4)	1.99(66)	0.005(3)	1.63(48)	0.010(2)	0.008(3)
2	0.34(13)	2.1(8)	0.004(4)	2.12(81)	0.006(3)	1.94(91)	0.015(4)	0.012(4)
3	0.75(6)	2.1(6)	0.004(2)	2.00(34)	0.005(2)	1.04(19)	0.007(1)	0.011(2)
4	0.74(9)	2.1(9)	0.003(3)	1.76(48)	0.003(2)	1.21(35)	0.009(2)	0.014(3)
15	0.89(15)	2.0(1.6)	0.007(9)	1.66(75)	0.005(4)	1.34(47)	0.008(3)	0.013(5)
19	1.26(13)	2.0(1.3)	0.010(11)	2.11(60)	0.010(11)	1.46(44)	0.009(2)	0.012(4)
25	1.34(15)	2.7(1.5)	0.013(12)	1.88(61)	0.005(3)	1.45(53)	0.010(3)	0.010(4)
30	1.20(7)	2.8(6)	0.003(2)	1.48(63)	0.004(2)	1.46(28)	0.009(2)	0.009(2)
40	1.29(11)	2.3(1.0)	0.005(5)	1.64(50)	0.005(3)	1.48(40)	0.009(2)	0.013(4)
46	1.32(10)	2.9(1.0)	0.011(6)	1.56(37)	0.004(2)	1.51(34)	0.009(2)	0.008(4)

Time/h	r_C/Å	r_S/Å	r_{Mo}/Å	r_N/Å	R (%)
0	2.162(13)	2.344(10)	2.801(5)	3.341(18)	37.47
2	2.154(18)	2.347(12)	2.806(9)	3.324(30)	40.55
3	2.141(10)	2.346(5)	2.786(3)	3.312(10)	24.24
4	2.143(17)	2.346(7)	2.783(5)	3.318(20)	31.56
15	2.159(24)	2.335(12)	2.767(7)	3.301(27)	44.77
19	2.185(28)	2.334(10)	2.770(6)	3.315(20)	35.55
25	2.183(29)	2.340(10)	2.776(7)	3.331(21)	40.74
30	2.159(7)	2.347(5)	2.777(4)	3.334(10)	27.56
40	2.183(16)	2.348(9)	2.780(5)	3.346(19)	34.39
46	2.169(15)	2.336(6)	2.773(4)	3.328(16)	26.96

N = Coordination number; r = interatomic distance; A = Debye–Waller factor; R = discrepancy index. r_O and A_O were fixed at 1.764 Å and 0.004 Å^2 (see text).

Table 2 Accounting for Mo (as % of total) in the species generated by Model A

	Coordination numbers				% Mo		
Time/h	N_O	N_C	N_S	N_{Mo}	$[MoO_4]^{2-}$	$[Mo_3S_4(CN)_9]^{5-}$	Total
0	0.00	2.59	1.99	1.63	0.0	81.3	81.3
2	0.34	2.12	2.12	1.94	8.4	97.1	105.5
3	0.75	2.07	2.00	1.04	18.8	52.2	71
4	0.74	2.05	1.76	1.21	18.5	60.3	78.8
15	0.89	2.00	1.66	1.34	22.2	67.0	89.2
19	1.26	2.03	2.11	1.46	31.6	72.9	104.5
25	1.34	2.69	1.88	1.45	33.4	72.7	106.1
30	1.20	2.77	1.11	1.46	30.1	73.2	103.3
40	1.29	2.28	1.64	1.48	32.3	74.1	106.3
46	1.32	2.87	1.56	1.51	33.0	75.3	108.3

The percentage of $[Mo_3S_4(CN)_9]^{5-}$ was calculated by dividing N_{Mo} by 2, and that of molybdenum in $[MoO_4]^{2-}$ obtained by dividing N_O by 4.

is possible to estimate that 0.8% of the Mo is present as $[MoS_4]^{2-}$ from the additional absorbance at 469 nm using the value $\varepsilon_{469} = 11186$ M^{-1} cm^{-1} determined from a solution of $[NH_4]_2[MoS_4]$. The percentage of Mo present in $[MoS_4]^{2-}$ is small enough to be neglected in the EXAFS data analysis to which we turned for further information about the other molybdenum species formed in the reaction.

EXAFS results

Model A. In model A the EXAFS data were fitted using five shells O, S, C, Mo and N with the minimum number of constraints. The occupation numbers N, distances r and thermal parameters A were refined for all but the oxygen shell (r_O at 1.764 Å and A_O at 0.004 Å^2 were fixed at values determined from the 46-hour data set) and the nitrogen shell where $N_N = N_C$, which is appropriate for CN groups. The overall energy zero, E_0, was also refined giving a total of 13 variables. It was necessary to include multiple scattering for the Mo–C–N unit without which the model calculated very little intensity for the high r peak in the Fourier transform. The Mo–C–N bond angle was fixed at 180° in order not to increase the number of variables, after trials showed that allowing it to vary made no significant differences to the fits. Table 1 gives the refined parameters with the errors calculated in the least-squares refinement. In Table 2 the amounts of Mo in the two species $[MoO_4]^{2-}$ and $[Mo_3S_4(CN)_9]^{5-}$ are calculated from N_O and N_{Mo}. The clearest feature is the increase in the percentage of molybdenum as molybdate, from zero at $t = 0$ to a maximum of about 30% reached after 19 hours. The percentage of $[Mo_3S_4(CN)_9]^{5-}$ also stabilises at around 70% after 19 hours and the total percentage of Mo in these two species is calculated to be close to 100%. Before 19 hours there must be other Mo containing species present because the total molybdenum calculated assuming only the species $[MoO_4]^{2-}$ and $[Mo_3S_4(CN)_9]^{5-}$ is less than 100%. However, it is difficult to determine what the other Mo containing species might be from the EXAFS refinements in Table 1. This is because the large number of variables used to fit the EXAFS data take up deficiencies in the model, which then appear as unreasonable temperature factors and occupancies.

Model B. In Model B it was assumed that the only Mo–S containing species was $[Mo_3S_4(CN)_9]^{5-}$ and that this was also the only species containing Mo–Mo bonds. This allowed the constraint $N_S = N_{Mo} \times 1.5$ to be added, in agreement with the formula $[Mo_3S_4(CN)_9]^{5-}$ since $N_S = 3$ and $N_{Mo} = 2$ in this cluster, and r_S, r_{Mo}, A_S and A_{Mo} to be fixed at the values determined for this cluster from the 46-hour EXAFS data. The results of the

Table 3 Structural parameters obtained from the molybdenum K-edge EXAFS study of the reaction between MoS_3 and KCN in aqueous solution (Model B)

Time/h	N_O	N_C	r_C/Å	A_C/Å²	N_{Mo}	r_N/Å	A_N/Å²	R (%)
0	0.00	4.8(1.5)	2.199(21)	0.017(8)	1.36(12)	3.325(16)	0.020(4)	44.89
2	0.66(14)	3.9(1.3)	2.161(22)	0.014(6)	1.30(12)	3.305(20)	0.020(5)	43.32
3	0.90(9)	3.7(9)	2.140(12)	0.016(4)	1.42(6)	3.306(11)	0.016(3)	28.69
4	0.86(12)	3.0(1.2)	2.145(20)	0.014(7)	1.46(9)	3.310(18)	0.023(4)	34.67
15	1.14(14)	2.1(1.3)	2.201(32)	0.016(14)	1.49(11)	3.318(23)	0.015(4)	45.33
19	1.30(13)	2.2(1.1)	2.196(23)	0.013(9)	1.52(10)	3.320(17)	0.013(3)	36.17
25	1.37(15)	2.9(1.6)	2.200(28)	0.021(15)	1.52(11)	3.332(22)	0.012(3)	41.31
30	1.20(9)	2.2(7)	2.179(17)	0.014(6)	1.43(7)	3.325(12)	0.013(2)	29.49
40	1.29(12)	2.1(1.0)	2.189(26)	0.012(9)	1.42(10)	3.329(18)	0.014(4)	35.95
46	1.31(10)	2.4(1.0)	2.198(21)	0.018(10)	1.46(8)	3.327(15)	0.013(3)	28.22

The following parameters were fixed: r_O (1.764 Å), A_O (0.004 Å²), r_S (2.333 Å) A_S (0.007 Å²), r_{Mo} (2.774 Å) and A_{Mo} (0.009 Å²) and $N_S = N_{Mo} \times 1.5$ (see text).

Table 4 Accounting for Mo (as % of total) in the species generated by Model B

	Coordination numbers				% Mo			
Time/h	N_O	N_C	N_{Mo}	N_C*	$[MoO_4]^{2-}$	$[Mo_3S_4(CN)_9]^{5-}$	$[Mo(CN)_8]^{4-}$	Total
0	0.00	4.80	1.36	2.75	0.0	68.4	34.4	102.8
2	0.66	3.90	1.30	1.93	16.5	65.7	24.1	106.3
3	0.90	3.70	1.42	1.57	22.5	71.0	19.6	113.1
4	0.86	3.00	1.46	0.81	21.5	73.0	10.2	104.7
15	1.05	2.15	1.49	−0.09	26.3	74.5	−1.1	99.7
19	1.30	2.15	1.52	−0.13	32.4	76.2	−1.7	107.0
25	1.37	2.89	1.52	0.60	34.1	76.1	7.5	117.8
30	1.20	2.19	1.42	0.06	29.9	71.2	0.7	101.8
40	1.29	2.11	1.42	−0.02	32.3	71.1	−0.3	103.1
46	1.31	2.35	1.46	0.16	32.8	73.0	2.0	107.8

$N_C^* = N_C - 1.5 \times N_{Mo}$ *i.e.* the value remaining after $[Mo_3S_4(CN)_9]^{5-}$ is accounted is used to calculate the amount of $[Mo(CN)_8]^{4-}$.

EXAFS refinements using these assumptions are shown in Table 3. There is a small increase in the *R*-factor values as would be expected from a large reduction in the number of variables used to fit the EXAFS signal. However, the parameters, for example thermal factors for carbon and nitrogen, obtained in the least-square refinements are now more physically realistic. Refinements using Model B reveal that at the start of the reaction there are on average 2.75 more CN groups attached to molybdenum than can be accounted for by the $[Mo_3S_4(CN)_9]^{5-}$ cluster. It is possible to account for these extra CN by assuming that a species $[Mo(CN)_x]^{n-}$ is present at the start of the reaction. A plausible species is octacyanomolybdate $[Mo^{IV}(CN)_8]^{4-}$ which has previously been reported as a by-product in the reaction between MoS_3 and cyanide by Müller *et al.*[13] Table 4 shows the accountancy for molybdenum assuming that the three species $[Mo(CN)_8]^{4-}$, $[Mo_3S_4(CN)_9]^{5-}$ and $[MoO_4]^{2-}$ account for the molybdenum K-edge EXAFS data. There is *a posteriori* support for the assumptions made in that the total molybdenum is found to be close to 100% for all the data sets. Examining Table 4 it appears that the $[Mo(CN)_8]^{n-}$ species is converted into $[MoO_4]^{2-}$. This is included in our final model.

Model C. In this model the assumption that the three species $[Mo(CN)_8]^{4-}$, $[Mo_3S_4(CN)_9]^{5-}$ and $[MoO_4]^{2-}$ could account for the molybdenum K-edge EXAFS data was incorporated using the rule that $C_{Mo}([Mo_3S_4(CN)_9]^{5-}) + C_{Mo}([Mo(CN)_8]^{4-}) + C_{Mo}([MoO_4]^{2-}) = 1$ where C_{Mo} is the fractional concentration of the various Mo containing species, for times up to and including 15 hours. This produced the constraint $N_C = 8 - (2.5 \times N_{Mo}) - (2 \times N_O)$. After 15 hours the constraint $N_C = 1.3 \times N_{Mo}$ was used, because all the cyanide containing molybdenum species other than $[Mo_3S_4(CN)_9]^{5-}$ have reacted to form molybdate.

The refined parameters for Model C are given in Table 5 and the derived percentages of each of the molybdenum containing species are given in Table 6. Fig. 5 shows how this model fits the three-hour data set when all three molybdenum containing

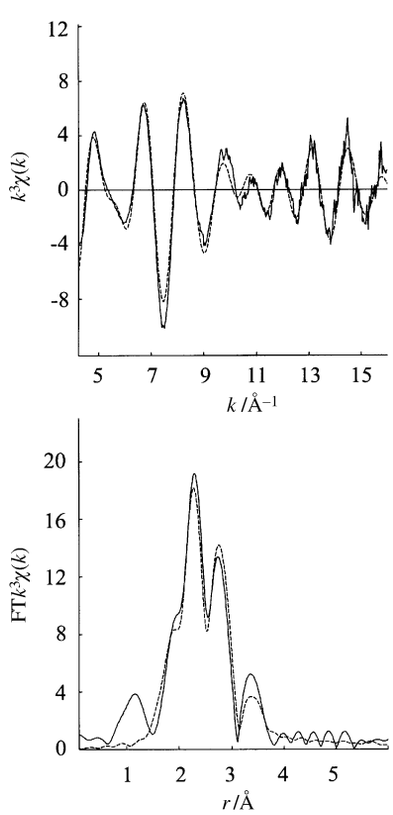

Fig. 5 Molybdenum K-edge EXAFS for MoS_3 + CN^- after 3 hours. Key as in Fig. 4.

Table 5 Structural parameters obtained from the molybdenum K-edge EXAFS study of the reaction between MoS_3 and KCN in aqueous solution (Model C)

Time/h	N_O	N_C	N_{Mo}	r_C/Å	r_N/Å	A_C/Å^2	A_N/Å^2	R (%)
0	0.00	*4.44*	1.43(13)	2.162(20)	3.316(19)	0.014(3)	0.023(2)	44.34
2	0.65(11)	*3.39*	1.33(11)	2.157(20)	3.303(17)	0.012(3)	0.020(4)	43.56
3	0.79(4)	*3.00*	1.37(5)	2.163(12)	3.309(9)	0.014(2)	0.019(2)	25.77
4	0.84(9)	*2.53*	1.51(8)	2.134(15)	3.314(17)	0.017(4)	0.017(4)	34.77
15	1.04(5)	*2.00*	1.41(10)	2.173(25)	3.301(15)	0.014(7)	0.011(4)	45.34
19	1.18(8)	*2.11*	1.41(5)	2.203(20)	3.319(15)	0.010(4)	0.014(3)	37.03
25	1.19(11)	*2.11*	1.40(6)	2.218(26)	3.328(17)	0.012(5)	0.014(3)	42.80
30	1.17(12)	*2.12*	1.41(3)	2.191(14)	3.326(8)	0.015(4)	0.012(1)	29.22
40	1.29(15)	*2.03*	1.35(4)	2.191(18)	3.326(13)	0.009(4)	0.013(2)	33.06
46	1.22(12)	*2.07*	1.39(4)	2.201(20)	3.324(12)	0.013(4)	0.014(2)	28.18

Parameters fixed: as in Table 3. N_C was constrained and calculated using $N_C = 8 - (2.5 \times N_{Mo}) - (2 \times N_O)$ for data sets up to and including 15 h and by $N_C = 1.3 \times N_{Mo}$ for all subsequent data sets (see text). N_C is listed because it is used in subsequent calculations.

Table 6 Accounting for Mo (as % of total) in the species generated by Model C

	Coordination numbers				% Mo		
Time/h	N_O	N_C	N_{Mo}	N_C*	$[MoO_4]^{2-}$	$[Mo(CN)_8]^{4-}$	$[Mo_3S_4(CN)_9]^{5-}$
0	0.00	*4.44*	1.43	*2.30*	0.0	28.6	71.4
2	0.65	*3.39*	1.33	*1.40*	16.2	17.3	66.5
3	0.79	*3.00*	1.37	*0.95*	19.7	11.8	68.5
4	0.84	*2.53*	1.51	*0.27*	21.1	3.4	75.5
15	1.04	*2.00*	1.41	*0.26*	26.1	3.2	70.7
19	1.18	*2.11*	1.41	*0.00*	29.5	0.0	70.5
25	1.19	*2.11*	1.40	*0.00*	29.8	0.0	70.2
30	1.17	*2.12*	1.41	*0.00*	29.3	0.0	70.7
40	1.29	*2.03*	1.35	*0.00*	32.4	0.0	67.7
46	1.22	*2.07*	1.39	*0.00*	30.6	0.0	69.4

N_C* = $N_C - 1.5 \times N_{Mo}$ *i.e.* the value remaining after $[Mo_3S_4(CN)_9]^{5-}$ is accounted for, and that used to calculate the amount of $[Mo(CN)_8]^{4-}$. In this model the total Mo is constrained to equal 100%.

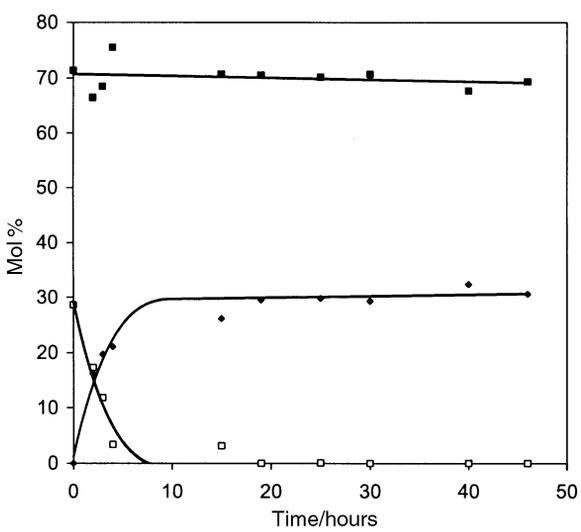

Fig. 6 Plot of the percentage of molybdenum in the three species $[Mo_3S_4(CN)_9]^{5-}$(■), $[Mo(CN)_8]^{n-}$ (□) and $[MoO_4]^{2-}$ (◆) *vs.* time in the reaction of MoS_3 + 9 CN^-. The curves are guides to the eye and have no kinetic significance.

species are present. The variation with time of the percentage of molybdenum in each of the three species $[Mo(CN)_8]^{4-}$, $[Mo_3S_4(CN)_9]^{5-}$ and $[MoO_4]^{2-}$ is shown in Fig. 6.

Infrared spectroscopy

Infrared spectra collected at the start of the reaction and after 24 hours are shown in Fig. 7. These show that a complex mixture of cyano species is formed at the start of the reaction, perhaps a mixture of $[M^{IV}(CN)_8]^{4-}$, $[M^{V}(CN)_8]^{3-}$,

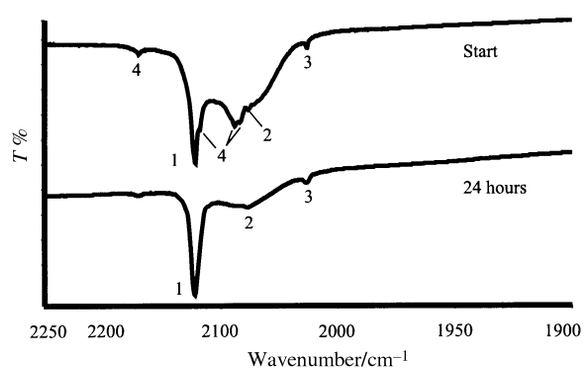

Fig. 7 The ν(CN) region of the infrared spectra of the solution produced by the reaction of MoS_3 with KCN. Features arise from the following species: 1 = $K_5[Mo_3S_4(CN)_9]$; 2 = KCN; 3 = KSCN; 4 = a mixture of $Mo(CN)_x$ species (spectra recorded as KBr pellets, see text).

$[M^{II}(CN)_7]^{5-}$ and $[Mo^{III}(CN)_7]^{4-}$. Unfortunately, in our EXAFS analysis we cannot differentiate between coordination number 7 and 8.

Implications for the structure of amorphous MoS_3

Combining the results of molybdenum K-edge EXAFS, UV-visible spectroscopy and infrared spectroscopy experiments has produced quantitative information on the molybdenum containing species produced in the reaction of aqueous cyanide with amorphous MoS_3. The most important result is that 70% of the molybdenum in MoS_3 is converted into Mo_3 clusters in solution on dissolution and that the concentration of these clusters does not change with time. This result has important implications for the structure of amorphous MoS_3. Assuming

that the reactions shown in Fig. 2 are close to quantitative[17] they suggest that MoS_3 contains 70% of the Mo in Mo–Mo bonded triangles.

Most of the remaining 30% of the molybdenum in MoS_3 is converted into mononuclear cyanomolybdate complexes that are oxidised to $[MoO_4]^{2-}$ over the course of the reaction. A very small (≈0.8%) amount of the molybdenum in MoS_3 is converted into $[MoS_4]^{2-}$ initially and then oxidised to $[MoO_4]^{2-}$. There is no evidence for the formation of dimeric molybdenum complexes in the EXAFS data. The UV-visible spectra are also consistent with the formation of mononuclear cyanomolybdenum complexes but not dinuclear molybdenum species, which have strong absorptions in the UV-visible.

The figure of 70% of molybdenum in Mo–Mo bonded Mo_3 clusters with the remaining Mo not participating in Mo–Mo bonding produces an average Mo–Mo coordination number (CN) of 1.4 for amorphous MoS_3. This figure is in excellent agreement with that from our neutron-diffraction study of MoS_3, Mo–Mo CN = 1.31(8) (assuming the pair correlations at 2.75 Å in the total correlation function obtained from the diffraction data arise solely from Mo–Mo),[11] and our most recent EXAFS study[20] in which we found the Mo–Mo coordination number to be 1.38(13). However, in our neutron diffraction study we reached very different conclusions on the structure of MoS_3. This was because we were attempting to determine if MoS_3 was built exclusively from Mo_3 Mo–Mo bonded structural units or if the experimental data were more compatible with chain models built from Mo–Mo bonded Mo_2S_9 units. Our neutron diffraction work excluded models in which all the molybdenum in amorphous MoS_3 was in Mo_3 groups and we therefore decided in favour of models based on molybdenum dimers. We also favoured chain models built from Mo–Mo bonded Mo_2S_9 units in our earlier EXAFS work[7,11] because we obtained Mo–Mo coordination numbers closer to one than two.

The present work suggests that models for MoS_3 based on only one type of unit are too simplistic. It supports Müller's idea that MoS_3 must contain Mo_3 triangles, but suggests, especially when combined with evidence from diffraction experiments, that these must be linked together by other types of structural units lacking Mo–Mo bonds.

Conclusion

Chemical excision combined with EXAFS suggests that in amorphous MoS_3 70% of the molybdenum is found in Mo–Mo bonded Mo_3 units and 30% in mononuclear Mo units. This result is shown to be consistent with the results of previous EXAFS and diffraction measurements, but contradicts previous conclusions on the structure of MoS_3. In previous work on MoS_3, authors, including ourselves, have reached conclusions on its structure because they assumed it must be built from only one type of structural unit. The results of this work should provide both a new starting point and check on the validity of extended structural models of amorphous MoS_3.

Obvious extensions of this work are the study of excision reactions of the amorphous molybdenum and tungsten sulfides, $MoS_{4.7}$, WS_3 and WS_5,[21,22] and the amorphous rhenium sulfide Re_2S_7.

Acknowledgements

We thank the EPSRC for the provision of EXAFS facilities and a studentship for M. R. F.

References

1 T. Weber, J. C. Muijsers and J. W. Niemantsverdriet, *J. Phys. Chem.*, 1995, **99**, 9194.
2 T. Weber, J. C. Muijsers, H. van Wolput, C. P. J. Verhagen and J. W. Niemantsverdriet, *J. Phys. Chem.*, 1996, **100**, 14144.
3 R. R. Chianelli, *Int. Rev. Phys. Chem.*, 1982, **2**, 127.
4 S. P. Cramer, K. S. Liang, A. J. Jacobson, C. H. Chang and R. R. Chianelli, *Inorg. Chem.*, 1984, **23**, 1215.
5 D. R. Huntley, T. G. Parham, R. P. Merril and M. J. Sienko, *Inorg. Chem.*, 1983, **22**, 4144.
6 R. A. Scott, A. J. Jacobson, R. R. Chianelli, W.-H. Pan, E. I. Stiefel, K. O. Hodgson and S. P. Cramer, *Inorg. Chem.*, 1986, **25**, 1461.
7 S. J. Hibble, D. A. Rice, D. M. Pickup and M. P. Beer, *Inorg. Chem.*, 1995, **34**, 5109.
8 K. S. Liang, S. P. Cramer, A. J. Jacobson, C. H. Chang, J. P. de Neufville, R. R. Chianelli and F. J. Betts, *J. Non-Cryst. Solids*, 1980, **42**, 345.
9 E. Z. Diemann, *Z. Anorg. Allg. Chem.*, 1977, **432**, 127.
10 F. Z. Chien, S. C. Moss, K. S. Liang and R. R. Chianelli, *Phys. Rev. B*, 1984, **29**, 4606.
11 S. J. Hibble, R. I. Walton, D. M. Pickup and A. C. Hannon, *J. Non-Cryst. Solids*, 1998, **232**–**234**, 434.
12 A. Müller, E. Diemann, E. Krickemeyer, H. J. Walberg, H. Bögge and A. Armatage, *Eur. J. Solid State Inorg. Chem.*, 1993, **30**, 565.
13 A. Müller, R. Jostes, W. Eltzner, C. S. Nie, E. Diemann, H. Bögge, M. Zimmermann, M. Dartmann, U. Reinschvogell, S. Che, S. J. Cyvin and B. N. Cyvin, *Inorg. Chem.*, 1985, **24**, 2872.
14 A. Müller, V. Fedin, K. Hegetschweiler and W. J. Amrein, *J. Chem. Soc., Chem. Commun.*, 1992, 1795.
15 A. Müller, S. Sarkar, R. G. Bhattacharyya, S. Pohl and M. Dartmann, *Angew. Chem., Int. Ed. Engl.*, 1978, **17**, 535.
16 A. Müller, W. Nolte and B. Krebs, *Angew. Chem., Int. Ed. Engl.*, 1978, **17**, 279.
17 A. Müller, *Angew. Chem., Int. Ed. Engl.*, 1980, **19**, 72.
18 A. Müller, E. Krickmeyer, H. Bögge, H. Ratajczak and A. Armatage, *Angew. Chem., Int. Ed. Engl.*, 1994, **33**, 770.
19 (*a*) EXCALIB: Daresbury Laboratory Computer Program; (*b*) M. Newville, P. Livins, Y. Yawby, E. A. Stern and J. J. Rehr, *Phys. Rev. B*, 1993, **47**, 14126; (*c*) N. Binsted, EXCURV 98, CCLRC Daresbury Laboratory, 1998.
20 R. I. Walton, A. J. Dent and S. J. Hibble, *Chem. Mater.*, 1998, **10**, 3737.
21 S. J. Hibble and M. R. Feaviour, unpublished results.
22 M. R. Feaviour, PhD Thesis, University of Reading, 1999.